American Journal of Energy Engineering
2018; 6(4): 50-56
http://www.sciencepublishinggroup.com/j/ajee
doi: 10.11648/j.ajee.20180604.13
ISSN: 2329-1648 (Print); ISSN: 2329-163X (Online)

Study of the Diffusion Capacity of a CIGS-based Solar Cell in Dynamic Frequency Regime Under Monochromatic Illumination: Effect of Incidence Angle and Gallium Doping Rate

Gérome Sambou[1, *], Amadou Diao[2], Jean Jude Domingo[2], Djimba Niane[2], Moustapha Dieng[2]

[1]Laboratory of Semiconductors and Solar Energy, Physics Department, Faculty of Science and Technology, University Cheikh Anta Diop, Dakar, Senegal

[2]Physics Department, Faculty of Science and Technology, University Cheikh Anta Diop, Dakar, Senegal

Email address:
sambougerome@yahoo.fr (G. Sambou), ama_diao@yahoo.fr (A. Diao), domingojean2001@yahoo.fr (J. J. Domingo), djimbasbn@gmail.com (D. Niane), moutaphadieng@hotmail.fr (M. Dieng)
[*]Corresponding author

To cite this article:
Gérome Sambou, Amadou Diao, Jean Jude Domingo, Djimba Niane, Moustapha Dieng. Study of the Diffusion Capacity of a CIGS-based Solar Cell in Dynamic Frequency Regime Under Monochromatic Illumination: Effect of Incidence Angle and Gallium Doping Rate. *American Journal of Energy Engineering*. Vol. 6, No. 4, 2018, pp. 50-56. doi: 10.11648/j.ajee.20180604.13

Received: December 5, 2018; **Accepted**: January 2, 2019; **Published**: January 28, 2019

Abstract: In this paper a study in dynamic frequency regime under monochromatic illumination was made on a CIGS-based solar cell model. After solving the continuity equation of the minority carriers, equation governing the diffusion capacitance of the solar cell are extracted. The study shows that increasing the wavelength in the visible increases the module of capacitance at a gallium doping rate X=0.3. On the other hand, the angle of incidence and the gallium doping rate decrease the module of diffusion capacitance. The study of the Bode diagram illustrated by the variation of the module of the capacitance and phase of the latter as a function of the logarithm of the pulsation shows the existence of two characteristic zones of the pulsation whose limit characterizes the dynamic regime The study shows that the pulsation limiting the static regime to the dynamic regime increases with the increase of the gallium doping rate.

Keywords: CIGS, Frequency Modulation, Wavelength, Incidence Angle, Gallium Doping Rate, Capacitance, Bode Diagram

1. Introduction

Copper indium gallium selenide (CIGS) of chalcopyrite crystalline structure has a band gap varying continuously with the molar ratio of indium from about 1.0 eV (for copper indium selenide) to about 1.7 eV (for copper gallium selenide), which is known as an alternative solar cell material. Recently, a number of fundamental and engineering studies of CIGS have been reported because of the importance of renewable energy. To link the characteristics of a thin-film solar cell with the properties of the CIGS material, theoretical study models have been made. Electrical parameters are determined in static mode [1], but also in dynamic mode [2] under monochromatic illumination. In thin-film solar cells, the diffusion phenomines at the CdS/CIGS junction make up most of the cell's performance. Thus the illumination of the solar cell causes a diffusion of excess minority carriers. The space charge region of a solar cell can be considered as a plane capacitor named transition capacitance [3].

These carriers, characterized by a lifetime in the base, are the source of the photocurrent and the photocurrent density. A study of the density of minority carriers, photocurrent density and phototension in dynamic frequency regime was previously carried out [4]. For this work, we show the effect of the wavelength, the incidence angle and the gallium doping rate on the diffusion capacitance of a CIGS solar cell.

2. Theoretical Study

The CIGS solar cell considered in this study is presented at the Figure 1.

Under the effect of an excitation (optical or electric), the charge carriers are generated in the base of the solar cell. Taking into account the generation phenomena, diffusion and recombination in the solar cell, the angle of incidence, the continuity equation of the minority carrier charge in the base in the frequency dynamic regime is given bay: [5, 6]

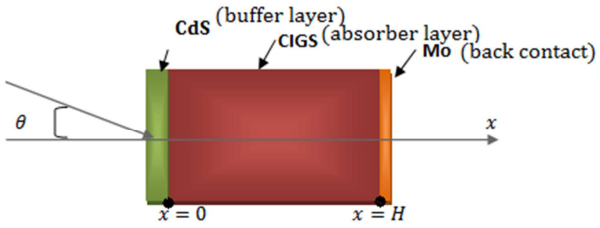

Figure 1. *Simplified schema of a CIGS-based solar cells with one dimensional dimensions.*

Where θ is the angle of incidence, H is the thickness of the base.

$$D(\omega).\frac{\partial^2\delta(x,\theta,t)}{\partial x^2}-\frac{\delta(x,\theta,t)}{\tau}=-G(x,\theta,t)+\frac{\partial\delta(x,\theta,t)}{\partial t} \quad (1)$$

With $D(\omega)$the complex diffusion coefficient of minority carriers; $\delta(x,\theta,t)$the density of minority carriers; $G(x,\theta,t)$ the generation rate of minority carriers [7, 8] and τ the average life of minority carriers.

The density and generation rate of minority carriers can be set respectively in the form [9, 10]:

$$\delta(x,\theta,t)=\delta(x,\theta)e^{(-i\omega t)} \quad (2)$$

$$G(x,\theta,t)=g(x,\theta)e^{(-i\omega t)} \quad (3)$$

Where $\delta(x,\theta)$ and $g(x,\theta)$ are the spatial component and $e^{(-i\omega t)}$ is the temporal component.

For illumination from the front face of the solar cell and depending on the angle of incidence, the spatial component of the generation rate is:

$$g(x,\theta)=\alpha(\lambda)\Phi(\lambda)(1-R(\lambda))cos\theta e^{-\alpha(\lambda)x} \quad (4)$$

Where $\alpha(\lambda)$ is the absorption coefficient at the wavelength λ; R (λ) is the reflection coefficient of the material,$\Phi(\lambda)$ the incident photon flux, and θ the incidence angle.

By replacing equations (2), (3) and (4) in equation (1) we get:

$$\frac{\partial^2\delta(x,\theta)}{\partial x^2}-\frac{\delta(x,\theta)}{L_\omega^2}+\frac{g(x,\theta)}{D_\omega}=0 \quad (5)$$

with

$$L_\omega=L_0\sqrt{\frac{(1-i\omega\tau)}{1+(\omega\tau)^2}} \quad (6)$$

L_0 intrinsic diffusion length

L_ω the complex diffusion length

The general solution of the preceding equation (5) is given by the relation (7).

$$\delta(x,\theta)=Acosh\left(\frac{x}{L_\omega}\right)+Bsinh\left(\frac{x}{L_\omega}\right)-\frac{\alpha(\lambda)\Phi(\lambda)(1-R(\lambda)).L_\omega^2.cos\theta}{D_\omega.(\alpha^2(\lambda)L_\omega^2-1)}e^{-\alpha(\lambda)x} \quad (7)$$

The constants A and B are determined from the following boundary conditions:[11]

(1) At junction x=0:

$$\left.\frac{\partial\delta(x,\theta)}{\partial x}\right|_{x=0}=\frac{SF}{D_\omega}\delta(0,\theta) \quad (8)$$

(2) on the rear face of the base (x=H):

$$\left.\frac{\partial\delta(x,\theta)}{\partial x}\right|_{x=H}=-\frac{SB}{D_\omega}\delta(H,\theta) \quad (9)$$

SF and SB denote the recombination speeds of the minority load carriers at the junction and rear face of the base respectively.

The expression of minority carriers density is expressed as a function of the CIGS absorption coefficient. This coefficient depends on gallium doping and is given by:

$$\alpha(\lambda,X)=A\sqrt{(\frac{hc}{\lambda}-E_g(X))} \quad (10)$$

with A (cm^{-1} $eV^{-1/2}$) a constant [12].

The following figure2 represents the variation of the energy of the CIGS gap as a function of the gallium doping rate.

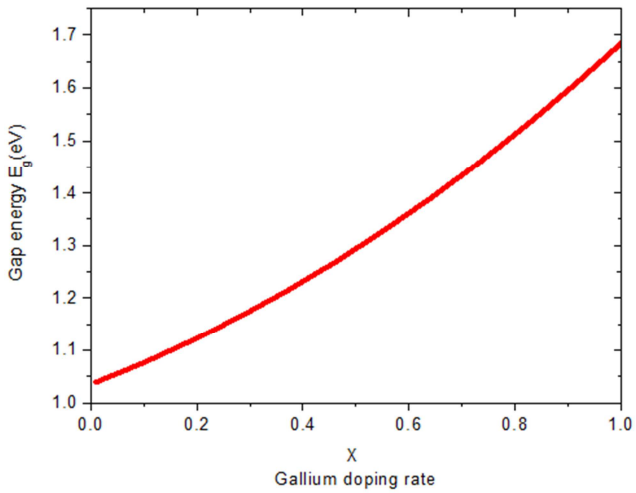

Figure 2. *Variation of the energy of the gap with the gallium doping rate.*

Figure II-2 shows the variation in gap energy as a function of the gallium doping rate. There is an increase in the energy of the E_g gap of the CIGS absorbent layer with the gallium doping rate. This evolution is also predicted by other authors [13, 14].

Figure II-3 shows the absorption coefficient as a function of wavelength for different gallium doping rates.

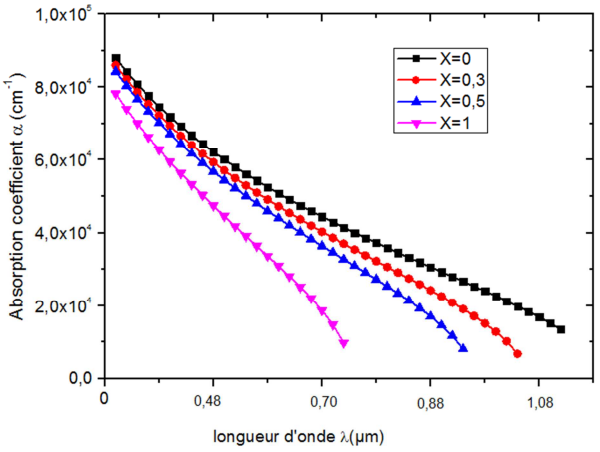

Figure 3. *Variation of the absorption coefficient with wavelength for different gallium doping rates.*

Figure II-3 shows the variation of the CIGS absorption coefficient as a function of wavelength for different gallium doping rates. There is a gradual decrease of the absorption coefficient in terms of wavelength. Indeed, for a given gallium doping rate, the low wavelengths (high energies) will correspond to a high absorption, hence the look of the curve.

Moreover, the four curves show that for a given wavelength, the increase of the doping rate leads to a decrease of the absorption coefficient. Indeed, our study already shows an increase in the energy of the CIGS gap as a function of the gallium doping rate (Figure 2). Thus the increase of the gag decreases the ratio energy incident energy of the gag, hence a decrease of the absorption coefficient.

Beyond the expressions of minority carriers density, photocurrent density and photovoltage are determined according to the angle of incidence of gallium doping rate, frequency and wavelength.

The photocurrent density is given by the following expression:

$$J(\lambda,\omega,SF,SB,\theta,X) = q.D_{\omega}.\frac{\partial\delta(x,\lambda,\omega,SF,SB,\theta,X)}{\partial x}\Big|_{x=0} \quad (11)$$

where q is the elementary charge.

From the excess minority carriers' density, we deduce the photovoltage across the junction, according to the Boltzmann's relation as follow

$$V(\lambda,\omega,SF,SB,\theta,X) = V_T ln[\frac{Nb}{n_0^2}\delta(0,\lambda,\omega,SF,SB,\theta,X)+1] \quad (12)$$

with V_T the thermal voltage, Nb the base doping density, n_0 the intrinsic carriers' density.

The charge variation in the base leads to a corresponding photovoltage variation across the junction; this gives rise to an associated capacitance. This capacitance is mainly due to the fixed ionized charge (dark capacitance) at the junction boundaries and the diffusion process (diffusion capacitance) [15, 16]

The solar cell's capacitance can be defined by:

$$C = \frac{dQ}{dV_{ph}} \quad (13)$$

with

$$Q = q.\delta((x,\lambda,\omega,SF,SB,\theta,X))|_{x=0} \quad (14)$$

The following expression (15) is obtained after calculation

$$C(x,\lambda,\omega,SF,SB,\theta,X) = \frac{q.n_0^2}{V_T.N_b} + \frac{q.\delta((0,\lambda,\omega,SF,SB,\theta,X))}{V_T} \quad (15)$$

From this expression it is clear that the capacitance is composed of two terms:

The first term expresses the intrinsic capacitance C_0; it depends on the nature of the material (substrate) through n_0, the doping of the material through (Nb) and the temperature through V_T and the gallium doping rate.

In the second term, of course, it depends on the temperature (V_T), the doping of the material and its nature (D and L), the operating point (Sf), the quality of the rear interface (Sb), the size of the photopile (H), the incident angle (θ) and the gallium doping rate. From this analysis of the expression of diffusion capacitance, it is easy to understand that it will be easily influenced by parameters such as wavelength, frequency, the incident angle and the gallium doping rate.

3. Results and Discussions

3.1. Diffusion Capacitance Profile: Wavelength Effect

Figure 4- below shows the module of diffusion capacitance as a function of recombination speed at the junction for different wavelength values.

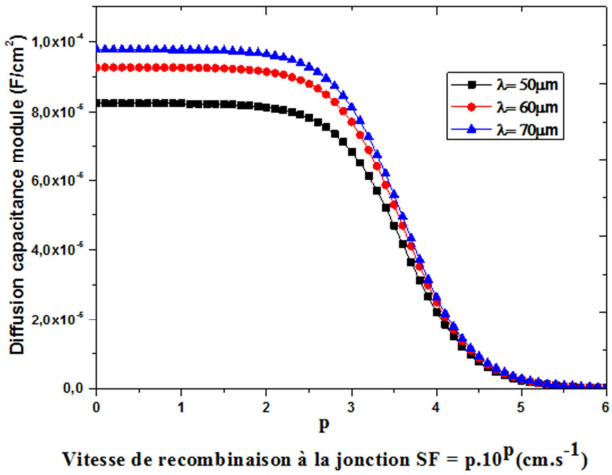

Figure 4. *diffusion capacitance module as a function of recombination rate at the junction for different wavelengths.*

$SB = 210^2\ cm/s$; $\omega = 3.10^3 rad.s^{-1}$; $\theta = 0°$ $X = 0{,}3$

These curves show that the capacitance module decreases with the recombination speed at the junction. Thus we distinguish two characteristic zones:

- first zone located in the vicinity of the open circuit: this zone with low recombination speed values corresponds to the maximum capacitance. Indeed, in the vicinity of the open circuit few excess minority load carriers in the base pass through the junction. Hence a significant charge storage in the space charge area.

-second zone corresponding to the high recombination speeds: here the capacitance suddenly decreases to finally tend towards the short-circuit capacitance. This sudden decrease is due to a rapid release of minority carriers in the base of the photopile.

Moreover, a deeper observation of the influence of wavelength in the visible allows us to observe that the more the wavelength increases, the more the amplitude of the photopile's capacitance module increases. Indeed, the increase in wavelength corresponds to a decrease in energy associated with radiation. This is an energy domain just necessary to stimulate inter-band transitions in the space load zone, resulting in an increase in the accumulation of charges, therefore that of the capacitance.

3.2. Diffusion Capacitance Profile: Incidence Angle Effect

Figure 5 shows the variation of the photopile capacitance module as a function of the recombination speed at the junction for different values of the angle of incidence.

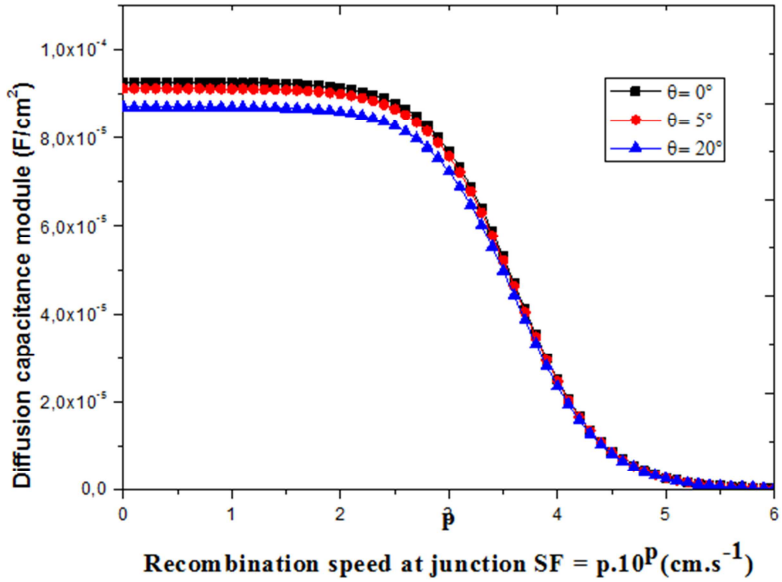

Figure 5. *Diffusion capacitance module as a function of the recombination speed at the junction for different values of the incidence angle.*

$SB = 210^2\ cm/s$; $\omega = 3.10^3 rad.s^{-1}$; $\lambda = 0{,}60\mu m$; $X = 0{,}3$

The capacitance remains constant and high for low values of the recombination speed at the junction and decreases to reach very low values towards high values of the recombination speeds at the junction. A decrease in capacitance is observed if the angle of incidence is increased. Indeed the decrease of the luminous intensity, the shading effects due to the metal grids and those of the ohmic contacts... are so many elements limiting a good generation of minority carriers. Thus we are witnessing a low generation of minority carriers, resulting in a slight decrease in carrier storage, and therefore a slight decrease in capacitance.

3.3. Diffusion Capacitance Profile: Gallium Doping Rate Effect

The following figure6 represents the variation of the capacitance module as a function of the recombination speed at the junction for different values of the gallium doping rate

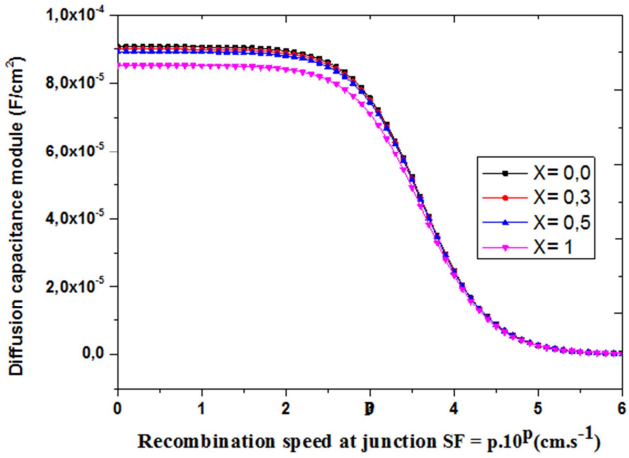

Figure 6. *Diffusion capacitance module as a function of recombination speed at junction for different gallium doping rate.*

$SB = 210^2\ cm/s$; $\omega = 3.10^3 rad.s^{-1}$; $\lambda = 0{,}60\mu m$; $\theta = 0$

For low values of the recombination speed at the junction,

the capacitance remains independent of the SF speed. It decreases very quickly to tend towards very low values. The increase in gallium doping rate decreases the module of capacitance. Indeed the increase of the gallium doping rate increases the area of space charge, hence the width of the capacitance. Thus we are witnessing an increase in recombination zones, resulting in a decrease in minority carriers and therefore a decrease in capacitance. Subsequently, the following results explain the Bode diagram [17] of the cell capacitance

3.4. Bode Diagram Capacitance of the Solar Cell: Incident Angle Effect

The following figure 7 shows the variation of the diffusion capacitance with logarithm of pulsation for different values of the incidence angle

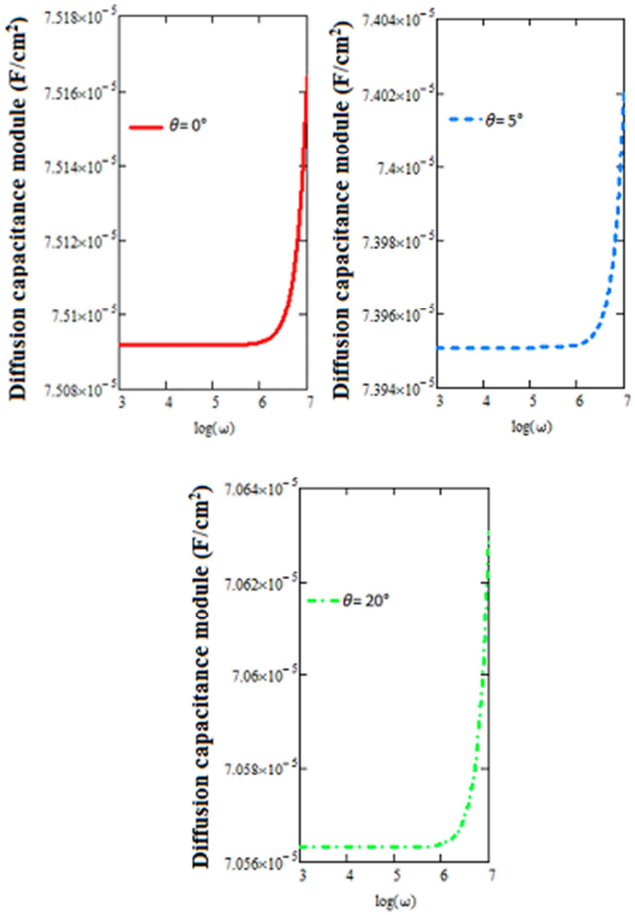

Figure 7. *Variation of the capacitance module with the logarithm of the pulsation for different values of the angle of incidence*

$SB = 210^2\ cm/s$; $SF = 3.10^3 cm/s$; $\lambda = 0{,}60\mu m$; $X = 0{,}3$

This figure 7 shows two characteristic pulsation zones.

A first zone $[0\,rad/s - 10^6 rad/s[$ in which the capacitance module does not change with pulsation. A second zone $[10^6 rad/s - 10^7 rad/s[$ where the diffusion capacitance module varies with pulsation. An increase that highlights the dynamic regime. Moreover, the increase of the incidence angle reduces the module of capacitance without affecting the frequency limiting the two zones mentioned above.

The following figure8 shows the variation of the capacitance phase as a function of the logarithm of the pulsation for different values of the incidence angle.

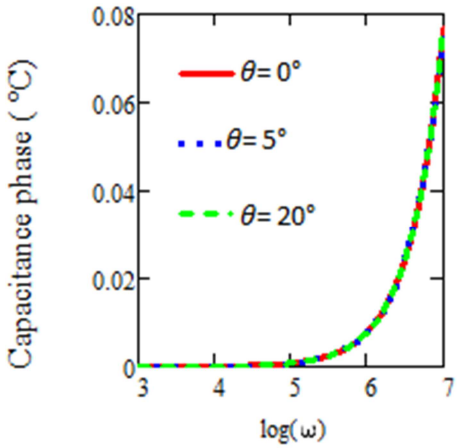

Figure 8. *Phase variation of the capacitance with the logarithm of the pulsation for different values of the angle of incidence*

$SB = 210^2\ cm/s$; $SF = 3.10^3 cm/s$; $\lambda = 0{,}60\mu m$; $X = 0{,}3$

This figure 8 shows the existence of two characteristic zones: a first zone$[0\ rad/s - 10^5 rad/s[$ in which the phase of capacitance does not vary with pulsation. A second zone $[10^5 rad/s - 10^7 rad/s[$ where the phase of the diffusion capacitance varies according to the pulsation. Thus in this second zone, there is phase shift between the incident signal and the carriers produced. Moreover, the increase in the angle of incidence does not affect either the phase of the capacitance or the frequency limiting the two zones mentioned above.

3.5. Bode Diagram Capacitance of the Solar Cell: Gallium Doping Rate Effect

Figure 9 shows the variation of the module of diffusion capacitance as a function of the logarithm of pulsation for different values of the gallium doping rate

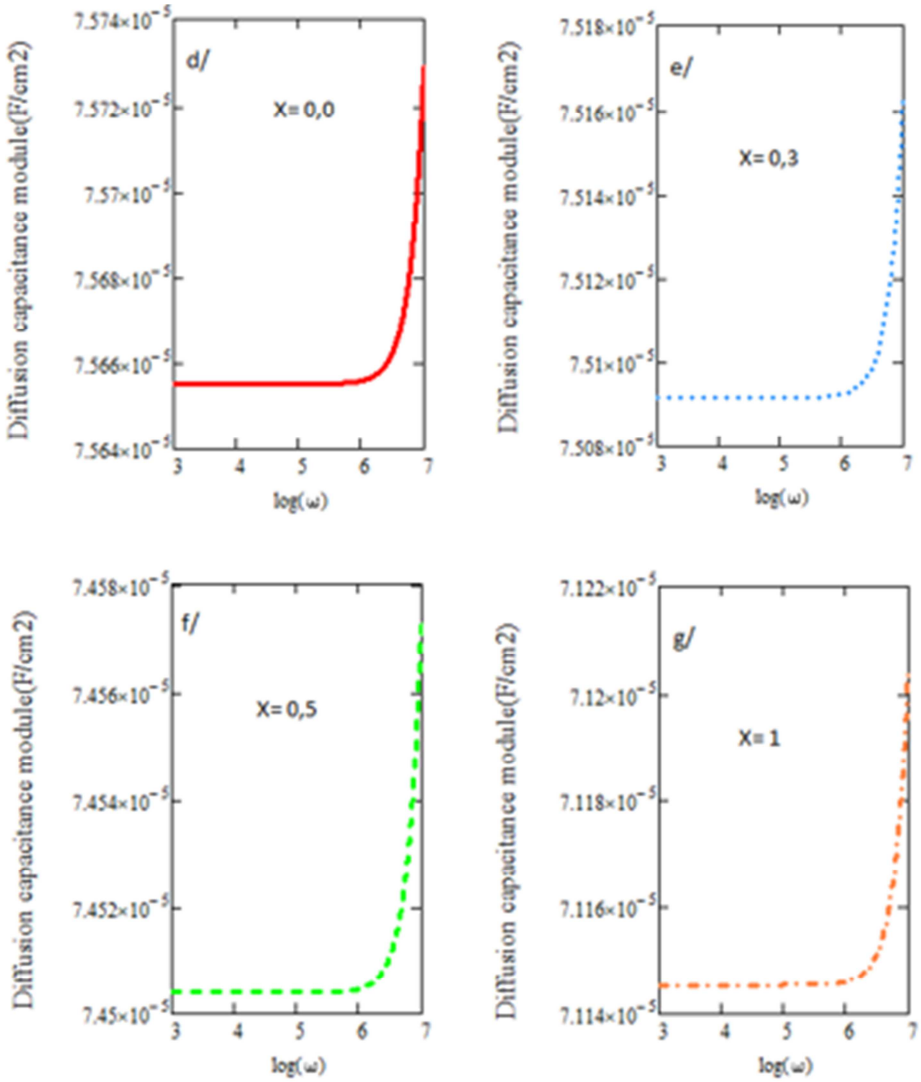

Figure 9. *Variation of the diffusion capacitance module with the logarithm of the pulsation for different values of the gallium doping rate.*

$SB = 210^2\ cm/s$; $SF = 3.10^3 cm/s$; $\lambda = 0{,}60\mu m$; ; $\theta = 0{,}0$

In this figure9 two characteristic pulsation zones are distinguished. A first zone$[0\ rad/s - 10^6 rad/s[$ where the capacitance module does not vary with pulse. A second zone $[10^6 rad/s - 10^7 rad/s[$ where the diffusion capacitance module varies according to the pulsation: this is the dynamic regime. Moreover, the gallium doping rate increase tends to decrease the module of capacity and also a slight increase in frequency limiting the two zone previously mentioned.

Figure 10 shows the phase variation of the capacitance as a function of the logarithm of the pulsation for different values of the gallium doping rate.

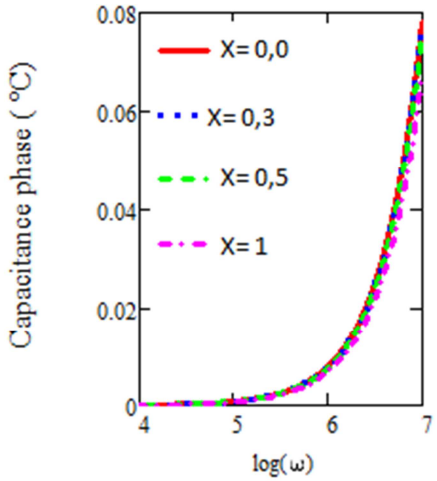

Figure 10. *Phase variation of the diffusion capacitance with the logarithm of the pulsation for different values of the gallium doping rate.*

$SB = 2.10^2\ cm/s$; $SF = 3.10^3 cm/s$; $\lambda = 0{,}60\mu m$; ; $\theta = 0$

Two zones are highlighted in this figure10: a first

zone $[0\,rad/s - 10^5 rad/s[$ in which the phase of capacitance does not vary with pulsation. A second zone $[10^5 rad/s - 10^7 rad/s[$ where the phase of the diffusion capacitance increased with pulsation. Thus there is phase shift between the incident signal and the carriers produced. Moreover, the increase in the doping rate with gallium decreases the phase of the capacitance but increases the frequency limiting the two previously mentioned zones.

In short, the study of the Bode diagram illustrated by the variation of the capacitance module as a function of the logarithm of the pulsation and that of the phase as a function of the logarithm of the pulsation highlights the predominance of inductive phenomena over the capacitive phenomena of our solar cell.

4. Conclusion

This article highlights the effects of wavelength, angle of incidence and gallium doping rate on the diffusion capacitance of a CIGS-based thin-film solar cell. Thus the increase of the wavelength in the visible increases the diffusion capacitance, that of the angle of incidence and the gallium doping rate decreases the capacitance. A study of the Bode diagram gives characteristic pulsation zones where the dynamic regime can be identified. It is also observed the influence of the gallium doping rate on the limit of the dynamic regime.

References

[1] Ibrahima WADE*, Mor NDIAYE, Alain Kassine EHEMBA, Demba DIALLO, Moustapha DIENG «Junction recombination velocity determination initiating the short-circuit and limiting the open circuit of a monofacialesolar cells containing thin film Cu (In, Ga)Se2 (CIGS) under horizontal illumination in static mode», IJESRT, 4 (9), (September, 2015).

[2] Jean Jude Domingo, Alain Kassine Ehemba, Demba Diallo, Ibrahima Wade and MoustaphaDieng. «Study of the capacity of a manofacial solar cell based on CIGS under horizontal monochromatic illumination in frequency dynamic mode: the effect of the wavelength» Int. J. Adv. Res. 4(11), (23 November 2016), 711-719.

[3] Chawla, G. B. R. and Gummel, H. K. «Transition Region Capacitance of Diffusion p-n Junction». IEEE Transactions on Electron Devices, 18, 178-195. http://dx.doi.org/10.1109/T-ED.1971.17172.

[4] Gerome SAMBOU*, Alain Kassine EHEMBA, Mouhamadou Mamour SOCE, Amadou DIAO, Moustapha DIENG «Frequency Modulation Study of a Monofacial Solar Cells Based on Copper Indium and Gallium Diselenide (CIGS) under Monochromatic Illumination: Influence of Incidence Angle and Gallium Doping» American Journal of Materials Science and Engineering, 2018, Vol. 6, No. 1, 7-11.

[5] N. Honma and C. Munakata, «Sample thickness dependence of minority carrier lifetimes measured using an ac photovoltaic method», Japan. J. Appl. Phys. 26,(1987) 2033-6.

[6] A. Dieng, I. Zerbo, M. Wade, A. S. Maiga et G. Sisoko, «Three-dimensional study of a polycrystalline silicon solar cell: the influence of the applied magnetic field on the elctrical parameters», Semicond. Sci. Technol. 26, (2011) pp: 5023-5032.

[7] J. N. Hollenhorst et G. Hasnain, « Frequency dependent whole diffusion in InGaAs double heterostructure » Appl. Phys. Lett, 65(15): (1995) 2203-2205.

[8] F. Ahmed et S. Garg, «simultaneous determination of diffusion length, lifetime and diffusion constant of minority carrier using a modulated beam» International Atomic Energy Agency. International centre for theorical physics. Internal report IC/86/129 , 1987.

[9] J. Dugas, «3D modelling of a reverse cell made with improved multicrystalline silicon wafers». Solar Energy Materials and Solar Cells Volume 32. Issue 1, (January 1994). Pages71-88.

[10] T. Flohr et R. Helbig, «Determination of minority-carrier lifetime and surface recombination velocity by Optical-Beam-Iduced-Current measurements at different light wavelengths» J. Appl. Phys. Vol. 66(7), (1989) pp 3060-3065.

[11] Sissoko, G., Museruka, C., Corréa, A., Gaye, I. and Ndiaye, «Light Spectral Effect on Recombination Parameters of Silicon Solar Cell. World Renewable Energy Congress, Part III» (1996), 1487-1490.

[12] Morales-Acevedo «Effective absorption coefficient for graded band-gap semiconductors and the expected photocurrent density in solar cells» Solar Energy Materials and Solar Cells 93(1): 41-44 January 2009.

[13] G. Hanna, A. Jasenek, U. Rau, and H. W. Schock, «Influence of the Ga-content on the bulk defect densities ofCu (In, Ga). Se_2» Thin Solid Films, 387, 71-73 (2001).

[14] Nima Khoshsirat, Nurul Amziah Md Yunus,∗, Mohd Nizar Hamidon, Suhaidi Shafie, Nowshad Amin «Analysis of absorber layer properties effect on CIGS solar cell performance using SCAPS» Optik 126 (2015) 681–686.

[15] Wenham SR, Green MA, Watt ME, Corkish R. Applied Photovoltaics. 2nd ed. ARC Centre for Advanced Silicon Photovoltaics and Photonics; 2007.

[16] Sane Moustapha, Sahin Gokhan, Barro Fabe drissa, Maiga Amadou Seidou. Incidence angle and spectral effects on vertical junction silicon solar cell capacitance. Turk J Phys 2014; 38: 221–7. http://dx.doi.org/10.3906/fiz-1311-9. TUB_ITAK.

[17] LATHI, BHAGWANDAS PANNALAL “Signals, systems and controls” Intext Educational Publisher, New York, 1973-1974.